SCIENCE CHINA
Technological Sciences

October 2010 Vol.53 No.10: 2853–2861
doi: 10.1007/s11431-010-4097-y

Application of polynomial chaos on numerical simulation of stochastic cavity flow

WANG XiaoDong[1,2] & KANG Shun[1*]

[1] *Key Laboratory of Condition Monitoring and Control for Power Plant Equipment, Ministry of Education, School of Energy Power and Mechanical Engineering, North China Electric Power University, Beijing 102206, China;*
[2] *Department of Mechanical Engineering, Vrije Universiteit Brussel, Brussels 1050, Belgium*

Received February 5, 2010; accepted July 7, 2010

In present paper, the mathematic background of intrusive polynomial chaos (IPC) method and coupling process with one dimension Euler equation were introduced. The IPC method was implemented for the 2D compressible stochastic Navier-Stokes equations to simulate the non-deterministic behavior of a lid driven cavity flow under the influence of uncertainties. The driven velocity and fluid viscosity were supposed respectively to be the uncertain variable which has Gaussian probability distribution. Based on the validation with benchmark results, discussions were mainly focused on the statistic properties of velocity distribution. The results indicated the effect of IPC method on the simulation of propagation of uncertainty in the flow field. For the simulated results of 2D cavity flow, influence of the driven velocity uncertainty is larger than that of viscosity.

non-deterministic, polynomial chaos, numerical simulation, lid driven cavity flow

Citation: Wang X D, Kang S. Application of polynomial chaos on numerical simulation of stochastic cavity flow. Sci China Tech Sci, 2010, 53: 2853–2861, doi: 10.1007/s11431-010-4097-y

1 Introduction

In past decades, the industrial application of computational fluid dynamics (CFD) had a great development [1]. The quality and credibility of industrial applications of CFD is one of the most attractive researching topics which have been developed rapidly in recent years. In 1998, AIAA proposed the guide for verification and validation of CFD simulation [2], in which two components are suggested: Firstly, the numerical error should be analyzed, called verification, to ensure the accuracy of numerical methodology; secondly, the simulation results should be compared with experiment data, called validation, to assess approximation of the numerical model used in CFD simulation to the real physical model. The sources of numerical error, such as grid density, computational domain scale, which exist mostly in CFD simulation, were listed in refs. [3, 4]. These error sources are the primary analytic objectives of the verification. For validation, the current view and procedure implemented by most researchers are the comparison between the simulated results and experimental results. Actually, it is far from satisfaction. For real physical problems, there are lots of non-determinis- tic factors which may have great influences on the performance, such as uncertain variation of geometry and working parameters, and uncertainty of boundary condition, working parameters and flow property, caused by manufacture process and working conditions. It should be noted that these factors mentioned above are different from the numerical error listed in refs. [3, 4]. However, investigation on the effects of all these factors has not been included in the current framework of CFD credibility research. The mathematic model and numerical methodology used widely are still deterministic, including deterministic flow parame-

*Corresponding author (email: kangs@ncepu.edu.cn)

ters, geometrical models and boundary conditions, with the aim of searching for the deterministic solution. Obviously, there will be great potential risks if only using such method in industrial design. If the performance of a design objective, such as turbine, compressor, aircraft, etc., is sensitive to some uncertain variable, even the minimal variation of the random variable could lead to catastrophic disaster. Therefore, in recent years, NASA and European Union launched a series of research projects [5, 6] for non-deterministic analysis methodology, firstly in aerospace research, to advance the robustness of design and analysis of complex system. Due to the high nonlinear property of control equation of fluid dynamics, complicated transition and turbulence models, it is more difficult to implement the non-deterministic method into fluid dynamics than solid mechanics. Thus, investigation on the non-deterministic methodology for CFD has been the main focus and difficulty in these research projects.

Non-deterministic analysis for CFD normally consists of two intimately components. The first one is involved in retrieving parametric uncertain property of random variable itself from the reliable data. Second one pertains to the influence of uncertain model input or model parameter on output parameters, namely propagation of uncertainty in flow field. Although, as can be concluded from experience of plenty of industry applications that the uncertain input or model parameters usually are stochastic variables with some certain probability distributions, it still needs a long term to accumulate a plenty of specific experiments and statistic processing to verify the distribution functions. Thus, it is far beyond the scope of present numerical analysis which mainly focuses on the second component. In other words, the non-deterministic physical problem can be treated as a stochastic process, and the distribution function of random variable is supposed to be known.

The traditional methods used to stochastic analysis can be divided into two types. One is statistic methods, such as Monte Carlo (MC) method, sampling method, etc.; the other is non-statistic methods, such as perturbation method, Neumann series expansion method, sensitive analysis, etc. The former is simple and can be easily used for many fields. But, usually, they are only used as the last resort since they are inefficient and normally need lots of samples which consume great computational resources. Perturbation and Neumann series expansion methods are limited to small perturbations and some simple cases. In recent years, some analysis methods based on spectral expansion were developed. Polynomial Chaos (PC) method is one of them. The basic theory of this method was proposed by Wiener [7], where it is called homogenous chaos. The pioneering development work of this method was done by Ghanem and Spanos in solid mechanics field [8]. In recent years, the applications of this method in fluid mechanics are expanded. Maitre simulated the 2D incompressible channel flow and convection flow in a cavity with uniform distributed viscosity coefficient [9]. Xiu and Karniadakis proposed the generalized polynomial chaos (GPC) method for different kinds of probability distribution functions. They found that there is an optimal polynomial corresponding to the specific probability distribution function, which ensures the exponential convergence [10]. Then, GPC was used in the simulation on stochastic incompressible channel flow and flow around cylinder [11]. Lacor et al. investigated the influence of stochastic boundary on 1D supersonic nozzle flow and the influence of stochastic viscosity coefficient on 2D cavity flow through coupling PC method with compressible Navier-Stokes equation [12]. Wu also simulated the cavity flow and back facing step flow with stochastic velocity boundary, but the application was limited to Stokes equation [13]. Wang and Kang solved the stochastic Burgers equation using PC method [14], and validated the results with analytical solution and results of Monte Carlo simulation. The comparison results showed the efficiency of the PC method is much higher than that of the MC method at the same accuracy level.

All the investigations mentioned above focused on the improvement and validity of PC method itself. However, the nature of physical problem simulated still remains unclear. The present work introduces the mathematic background of the PC method and the coupling process with control equation of fluid dynamic. The 2D lid driven cavity flows with stochastic driven velocity and viscosity are simulated and the discussions are focused on the variation of flow structure.

2 Mathematic models

According to the way of coupling with a CFD solver, the polynomial chaos method can be divided into non-intrusive and intrusive methods. In the non-intrusive polynomial chaos method (NIPC), the existing deterministic solver can be used as an encapsulated module without any changes. By implementing deterministic numerical simulation on some certain samples in stochastic space, then the statistic properties can be retrieved through statistic post processing on the results of deterministic simulation. Therefore, NIPC method requires no modifications to the verified CFD code, which prevents potential risks of introducing new error sources. The computational cost of NIPC depends on the number of samples. Although NIPC has the advantage of being several orders of magnitude cheaper than Monte Carlo method, it is still time consuming if the number of random variables is large. Moreover, the results obtained by this method are not unique, depending on the sampling method and distribution of samples. On the contrary, for the intrusive polynomial chaos (IPC) method, the control equations of fluid dynamic must be changed and lots of modifications must be implemented to the existing solver. However, the statistic properties of flow field can be built during the computational

process in one run. Therefore, it is much cheaper than NIPC, which is interesting from a practical point of view for CFD application. Hence, only IPC is introduced in the present paper. For minimizing the complicated mathematic formula, only one dimension Euler equation is used to demonstrate the procedure of building stochastic control equation of fluid dynamic. It is easy to extend it to the three-dimensional Navier-Stokes equations.

2.1 Polynomial expansion of stochastic variables

For a conventional deterministic problem, the flow parameters are real-valued functions of time t and space x. The support domain of these functions is denoted by D. If the flow problem has a stochastic process with some parameters being random variables, then the flow parameters will be functions of stochastic variables. Then these flow parameters are also stochastic variables. To avoid confusion, the variables introducing uncertainty into the flow fields are named random variables, which are usually regarded as input parameters of the stochastic flow model. Other flow parameters, regarded as output variables of the flow model, are named response variables.

The stochastic property of random variables and response variables can be represented by introducing an extra probability dimension into the flow model. Consider a probability space denoted by (Ω, F, P), where Ω denotes the sample space composed of basic outcomes, called the sample space. F is the σ-algebra of Ω, and P is the probability measure defined on the measurable space (Ω, F). The basic event in Ω is denoted by θ which doesn't depend on the specific physical property. The random variables and response variables are the events in Ω, which are the sets of basic events.

The function space mapping Ω onto R is denoted by Θ, each mapping $\Omega \to R$ is a random variable. A stochastic flow process is a square-integrable function defined on the product space $D\times\Omega$ since any random physical problem should be the process with finite-energy. Then, Θ is a Hilbert space with respect to L^2 norm. Let $\xi = \{\xi_1(\theta), \xi_2(\theta), \cdots, \xi_n(\theta)\}$ be a set of orthogonal and uncorrelated random variables in Θ, and $\varphi_k(\xi)$ be a polynomial in Θ. $\widehat{H}_p$ denotes the linear space composed of all polynomials $\varphi_k(\xi)$ with order less than p. Let $\overline{H}_p$ denote the closure of $\widehat{H}_p$ in Θ, and Ψ_p be the set of all polynomials in $\overline{H}_p$ and be orthogonal to $\overline{H}_{p-1}$. Then, the space spanned by Ψ_p, written in H_p, is named homogenous chaos of order p, which is a completed subspace of Θ. Ψ_p is a orthogonal basis of H_p, called polynomial chaos of order p. Then, any random variable $\varphi(\theta)$ in Θ can be approximated with the following representation:

$$\varphi(\theta) = \varphi_0 + \sum_{k=1}^{n} \varphi_k \Psi_1(\xi_k) + \sum_{k=1}^{n}\sum_{j=1}^{k} \varphi_{kj} \Psi_2(\xi_k, \xi_j) + \sum_{k=1}^{n}\sum_{j=1}^{k}\sum_{l=1}^{j} \varphi_{kjl} \Psi_3(\xi_k, \xi_j, \xi_l) + \cdots. \tag{1}$$

Rewrite it compactly as

$$\varphi = \sum_{k=1}^{N_{PC}} \varphi_k \Psi_k(\Xi). \tag{2}$$

The coefficient φ_k is deterministic. N_{PC} is the total number of polynomials in the expansions, which can be calculated by the following formula:

$$N_{PC} = \frac{(p+n)!}{p!n!} - 1, \tag{3}$$

where p is the order of polynomial chaos, and n is the number of random variables. The cumulative distribution function or probability density function of random variable is settled by the physical problem, and therefore, the coefficients of polynomials are known. For response variables, the coefficients are unknown and to be solved. The orthogonal property of polynomial in eq. (2) is defined by inner product with respect to a weighting function $\omega(\xi_1, \cdots, \xi_n)$:

$$\left\langle \Psi_i, \Psi_j \right\rangle = \int \Psi_i(\xi_1, \cdots, \xi_n) \Psi_j(\xi_1, \cdots, \xi_n) \omega(\xi_1, \cdots, \xi_n) \mathrm{d}\xi_1 \cdots \mathrm{d}\xi_n \triangleq \delta_{ij}.$$

Selection of the type of polynomials in eq. (2) depends on the probability density function of random variable. According to the Askey principle, an optimal polynomial chaos exists which is corresponding to the distribution function of random variable. The optimal means that the polynomial chaos will keep the exponential convergence rate if the weighting function is same as the probability density function [10]. For random variable in Gaussian, the probability density function is given by

$$f_\xi(\xi) = \frac{1}{\sqrt{2\pi}} \mathrm{e}^{-\frac{\xi^2}{2}}. \tag{4}$$

Thus, the optimal polynomial is Hermite polynomials with weighting function:

$$\omega(\xi_1, \cdots, \xi_n) = \frac{1}{\sqrt{2\pi}} \mathrm{e}^{-\frac{\xi_1^2 + \cdots + \xi_n^2}{2}}.$$

The one dimension Hermite polynomials are given as follows, which is used in the present paper:

$$\begin{cases} \Psi_0 = 1, \\ \Psi_1 = \xi, \\ \Psi_{p+1} = 2\xi\Psi_p(\xi) - 2p\Psi_{p-1}(\xi), \qquad p = 1, 2, \cdots. \end{cases} \tag{5}$$

2.2 Coupling process with Euler equation

One dimension unsteady Euler equations can be written as follows:

$$\frac{\partial \rho}{\partial t}+\frac{\partial \rho u}{\partial x}=0, \tag{6}$$

$$\frac{\partial \rho u}{\partial t}+\frac{\partial \rho u^2}{\partial x}=-\frac{\partial p}{\partial x}, \tag{7}$$

$$\frac{\partial \rho E}{\partial t}+\frac{\partial \rho u E}{\partial x}=-\frac{\partial p u}{\partial x}, \tag{8}$$

$$\rho E=\frac{p}{\gamma-1}+\frac{\rho u^2}{2}, \tag{9}$$

where u, ρ, p and E denote the velocity, density, static pressure and total energy, respectively. Expanding all these physical quantities using eq. (2), one has

$$\rho\left(t,x,\xi_1,\cdots,\xi_n\right)=\sum_{k=0}^{N_{pc}}\rho_k\Psi_k, \tag{10}$$

$$u\left(t,x,\xi_1,\cdots,\xi_n\right)=\sum_{k=0}^{N_{pc}}u_k\Psi_k, \tag{11}$$

$$p\left(t,x,\xi_1,\cdots,\xi_n\right)=\sum_{k=0}^{N_{pc}}p_k\Psi_k, \tag{12}$$

$$\rho E\left(t,x,\xi_1,\cdots,\xi_n\right)=\sum_{k=0}^{N_{pc}}(\rho E)_k\Psi_k. \tag{13}$$

The coefficients on the right sides of the expansions listed above are deterministic. The stochastic property of physical parameters is transferred to the polynomial of random variable, and the stochastic information is propagated by self-organization of chaos. Replacing the physical parameters in Euler equations (eqs. (6)–(9)) with the expansions (eqs. (10)–(13)) and applying Galerkin projection to each of the equation, one has the coupled Euler equations:

$$\frac{\partial \rho_k}{\partial t}+\sum_{i=0}^{N_{PC}}\sum_{j=0}^{N_{PC}}M_{ijk}\frac{\partial \rho_i u_j}{\partial x}=0,\ k=0,\cdots,N_{PC}, \tag{14}$$

$$\sum_{i=0}^{N_{PC}}\sum_{j=0}^{N_{PC}}M_{ijl}\frac{\partial \rho_i u_j}{\partial t}+\sum_{i=0}^{N_{PC}}\sum_{j=0}^{N_{PC}}\sum_{k=0}^{N_{PC}}L_{ijkl}\frac{\partial \rho_i u_j u_k}{\partial x}=-\frac{\partial p_l}{\partial x},\quad l=0,\cdots,N_{PC}, \tag{15}$$

$$\frac{\partial\left(\rho E\right)_k}{\partial t}+\sum_{i=0}^{N_{PC}}\sum_{j=0}^{N_{PC}}M_{ijk}\frac{\partial\left(\rho E\right)_i u_j}{\partial x}=-\sum_{i=0}^{N_{PC}}\sum_{j=0}^{N_{Pc}}M_{ijk}\frac{\partial p_i u_j}{\partial x},\quad k=0,\cdots,N_{PC}, \tag{16}$$

$$p_l=\left(\gamma-1\right)\left[\left(\rho E\right)_l-\sum_{i=0}^{N_{PC}}\sum_{j=0}^{N_{PC}}\sum_{k=0}^{N_{PC}}L_{ijkl}\frac{\rho_i u_j u_k}{2}\right],\ l=0,\cdots,N_{PC}, \tag{17}$$

where

$$\begin{cases}M_{ijk}=\dfrac{\left\langle\Psi_i\Psi_j\Psi_k\right\rangle}{\left\langle\Psi_k^2\right\rangle},\\ L_{ijkl}=\dfrac{\left\langle\Psi_i\Psi_j\Psi_k\Psi_l\right\rangle}{\left\langle\Psi_l^2\right\rangle}.\end{cases} \tag{18}$$

The inner product and triple inner product can be replaced by compact formats, i.e.,

$$\left(\rho u\right)_k=\sum_{i=0}^{N_{PC}}\sum_{j=0}^{N_{PC}}M_{ijk}\rho_i u_j,$$

$$\left(pu\right)_k=\sum_{i=0}^{N_{PC}}\sum_{j=0}^{N_{PC}}M_{ijk}p_i u_j,$$

$$\left(\rho u^2\right)_k=\sum_{i=0}^{N_{PC}}\sum_{j=0}^{N_{PC}}\sum_{k=0}^{N_{PC}}L_{ijlk}\rho_i u_j u_k,$$

$$\left(\rho u E\right)_k=\sum_{i=0}^{N_{PC}}\sum_{j=0}^{N_{PC}}M_{ijk}(\rho E)_i u_j.$$

Then, the stochastic Euler equations can be rewritten as follows.

$$\frac{\partial \rho_k}{\partial t}+\frac{\partial(\rho u)_k}{\partial x}=0, \tag{19}$$

$$\frac{\partial(\rho u)_k}{\partial t}+\frac{\partial\left(\rho u^2\right)_k}{\partial x}=-\frac{\partial p_k}{\partial x}, \tag{20}$$

$$\frac{\partial(\rho E)_k}{\partial t}+\frac{\partial(\rho u E)_k}{\partial x}=-\frac{\partial(pu)_k}{\partial x}, \tag{21}$$

$$p_k=(\gamma-1)\left[(\rho E)_k-\frac{(\rho u^2)_k}{2}\right],\quad k=0,\cdots,N_{PC}. \tag{22}$$

Solving eqs. (19)–(22) with the finite volume method or other numerical method obtains the deterministic coefficients of eqs. (10)–(13).

Using the same processing approach, stochastic Navier-Stokes equations can be built easily, which will not be presented here. However, it should be noted that the computational cost for solving eqs. (19)–(22) increases greatly compared to that for solving deterministic equations due to the increase of number of equations. For instance, when using the second-order polynomial chaos method for stochastic problem with one uncertain variable, N_{PC} will be 2, which means the number of equations will be double; while for the problems with 2 and 3 uncertain variables, the numbers of equations will increased by 5 and 9 times, respectively, which are still affordable for the current computational resources. However, according the comparison in ref. [14], the computational cost of polynomial chaos method is lower by approximately one order than that of Monte Carlo method when the dimension of the uncertainty is not very high.

2.3 Post processing of statistic properties

The coefficients of polynomial chaos expansion of response variables have been settled as shown above, and then they can be used to represent the statistic property of response variables.

2.3.1 Cumulative distribution function of response variables

Since ξ and θ are random variables, and ξ is the function of θ, the relationship between ξ and θ can be written as

$$f_\xi(\xi)\mathrm{d}\xi = f_\theta(\theta)\mathrm{d}\theta, \tag{23}$$

where f_ξ and f_θ denote the probability density functions of ξ and θ.

Since the response variable φ is the function of ξ and θ is distributed uniformly in [0, 1] [8], then,

$$f_\varphi(\varphi) = f_\xi(\xi)\mathrm{d}\xi = f_\theta(\theta)\mathrm{d}\theta = \mathrm{d}\theta. \tag{24}$$

After integration,

$$F_\varphi(\varphi(\theta)) = F_\xi(\xi(\theta)) = \theta, \tag{25}$$

where $F\varphi$ and F_ξ are the cumulative distribution function of φ and ξ. Since ξ is supposed to be in Gaussian distribution in this paper, eq. (25) can be rewritten by

$$\theta = F_\xi(\xi) = \frac{1}{\sqrt{2\pi}}\int_{-\infty}^{\xi} \mathrm{e}^{-\frac{t^2}{2}}\mathrm{d}t = \frac{1}{2}\left[1+\mathrm{erf}\left(\frac{\xi}{\sqrt{2}}\right)\right]. \tag{26}$$

Eqs. (25) and (26) build the relationship between ξ and F_φ. Since the relationship between φ and ξ is built by eq. (2), F_φ can be easily obtained from eqs. (2) and (26) since φ_k has been settled.

2.3.2 Mean value and standard deviation of response variables

According to the definition of the mean value

$$\overline{\varphi} = E[\varphi] = \int_{D_\varphi} \varphi f_\varphi(\varphi)\mathrm{d}\varphi, \tag{27}$$

where D_φ is the support domain of φ. From eqs. (2), (5) and (24), due to the orthogonal property of Hermite polynomial, the integration can be addressed by

$$\begin{aligned}
\overline{\varphi} &= \int_{D_\xi} \varphi f_\xi(\xi)\mathrm{d}\xi \\
&= \int_{D_\xi}\left(\sum_{k=0}^{N_{PC}} \varphi_k \Psi k(\xi)\right) f_\xi(\xi)\mathrm{d}\xi \\
&= \varphi_0\int_{D_\xi} \Psi_0(\xi) f_\xi(\xi)\mathrm{d}\xi + \sum_{k=1}^{N_{PC}} \varphi_k \int_{D_\xi} \Psi_k(\xi) f_\xi(\xi)\mathrm{d}\xi \\
&= \varphi_0 + \sum_{k=1}^{N_{PC}} \varphi_k \int_{D_\xi} \Psi_0(\xi)\Psi_k(\xi) f_\xi(\xi)\mathrm{d}\xi \\
&= \varphi_0,
\end{aligned}$$

where D_ξ is the support domain of ξ. It is found that the mean value of response variables is the zero order item of polynomial chaos. The standard deviation of the response variable can be addressed easily by

$$\begin{aligned}
\sigma_\varphi^2 &= E\left[\left(\varphi - E[\varphi]\right)^2\right] \\
&= \int_{D_\varphi} \left(\varphi - \overline{\varphi}\right)^2 f_\varphi(\varphi)\mathrm{d}\varphi \\
&= \int_{D_\xi} \left(\varphi - \varphi_0\right)^2 f_\xi(\xi)\mathrm{d}\xi \\
&= \int_{D_\xi} \left[\left(\sum_{i=0}^{N_{PC}} \varphi_i \Psi_i\right)\left(\sum_{j=0}^{N_{PC}} \varphi_j \Psi_j\right) - 2\varphi_0 \sum_{i=0}^{N_{PC}} \varphi_i \Psi_i + \varphi_0^2\right] f_\xi(\xi)\mathrm{d}\xi \\
&= \sum_{i=0}^{N_{PC}}\sum_{j=0}^{N_{PC}} \int_{D_\xi} \Psi_i \Psi_j f_\xi(\xi)\mathrm{d}\xi - \varphi_0^2 \\
&= \sum_{i=0}^{N_{PC}} \varphi_i^2 \left\langle \Psi_i^2 \right\rangle - \varphi_0^2 \\
&= \sum_{k=1}^{N_{PC}} \varphi_k^2 \left\langle \Psi_k^2 \right\rangle.
\end{aligned}$$

The high order statistic moments of response variables can be obtained using a similar processing.

3 Numerical method

3.1 Mesh and boundary condition

The computation domain is a square cavity, $0 \leqslant x, y \leqslant 1$. A structured mesh consisted of uniform 33×33 grid points is employed. All the walls (x=0, 1; y=0, 1) are no-sliding. The Reynolds number is set to 100 so that the flow can be considered as laminar. The dimensionless viscosity coefficient γ is 0.01. The velocity components in x and y directions are denoted by u and v, respectively. The upper wall is moving with a dimensionless velocity u=1.

3.2 Computation method

The 2D stochastic Navier-Stokes equation can be built by applying the same method presented in the last section to the 2D Navier-Stokes equation. The cell-centered finite volume method with second-order centered scheme is adopted. The time marching is performed in a low storage explicit four-stage Runge-Kutta scheme.

4 Simulated results and discussions

In a practical physical problem, there often exist several uncertainties simultaneously. However, it is difficult to distinguish clearly the influence of a certain uncertainty on the flow field if the coupled effects exist. Therefore, in the pre-

sent paper, the flow field with only one uncertainty is considered.

Two simulations with different random variables were computed under steady laminar flow condition.

Simulation 1. Set the lid driven velocity as a random variable, to investigate the influence of uncertainty of boundary conditions. The mean value of dimensionless lid driven velocity is set to 1 with a standard deviation of 10% of the mean value; the dimensionless viscosity coefficient γ = 0.01.

Simulation 2. Set viscosity coefficient as the random variable to investigate the influence of uncertainty of fluid's property. The lid driven velocity is constant, u =1; three levels, 0.01, 0.05 and 0.1, are set to be the mean values of viscosity coefficient, respectively with a standard deviation of 10% of each of the mean value.

4.1 Results of simulation 1

Figure 1 depicts the streamline pattern of statistic mean value of the flow field, in which the flow structure is quite similar to the results of deterministic simulation. As can be seen, three vortexes are formed in the flow field. The largest one, called main vortex, is close to lid with vortex core locating at the upper right side of center of the cavity. The other two corner vortexes, which are much smaller, locate at the lower corners of two sides of the cavity. This pattern shows the typical flow structure of lid driven cavity flow at Re = 100. The discussion will not be focused on this flow structure since it has been discussed extensively in references, such as refs. [15, 16].

Figure 2 shows the distribution of mean values of velocity components, u and v, on the central line of the cavity (y=0.5). For comparison, the deterministic benchmark value of v from ref. [15] is also shown in this figure. There is no doubt that an excellent agreement between the mean value and benchmark data is obtained. The probability density function of Gaussian random variable is symmetric with respect to mean value. Due to the influence of main vortex, v fluctuates about the central line with two peaks at the two sides of vortex core of the main vortex, whereas only one perk exists for u. The standard deviation of velocity component is used as error bar to demonstrate the uncertainty range. From the range of error bar, it can also be seen that the uncertainty will propagate from boundary to inside of the cavity. However, the error bar is not uniformly distributed. The peak of error is at the place where the peak of velocity component is located. The distributions of mean values and standard deviations of u and v on vertical central line (x=0.5) are shown in Figure 3. The positions of peaks of mean values and standard deviations overlap again. The

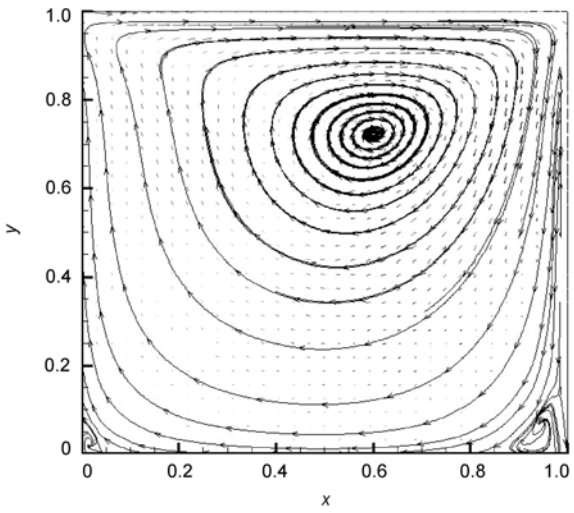

Figure 1 The streamline pattern of mean values.

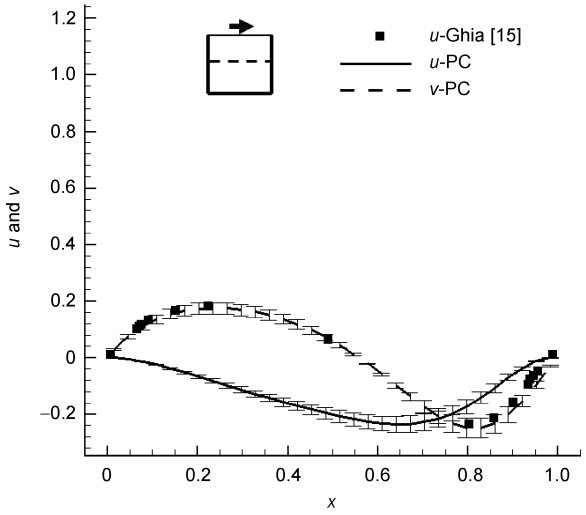

Figure 2 The distributions of mean values and standard deviations of velocity components at y = 0.5.

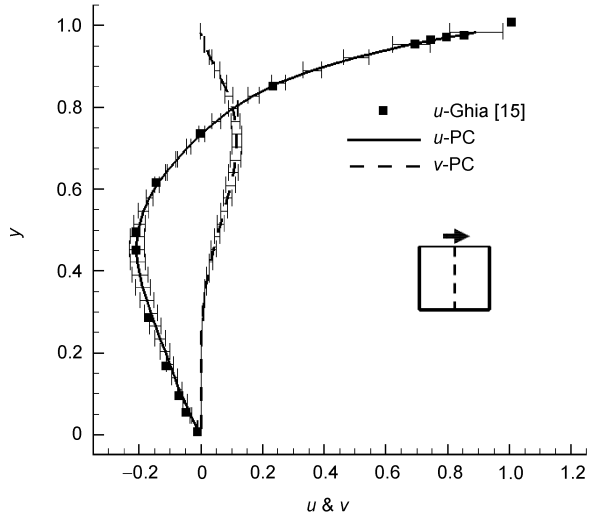

Figure 3 The distributions of mean values and standard deviations of velocity components at y = 0.5.

max error locates at the upper boundary, where the influence of uncertainty is the biggest. With increasing of the distance to uncertain boundary, the standard deviation decreases firstly, and then reaches another peak at about y=0.45.

The contours of standard deviations of velocity components in flow field, u and v, are shown respectively in Figures 4 and 5. The global max standard deviation of u is 0.1, locating at the upper boundary. Another peak with value 0.027 locates below the vortex core of the main vortex. The distribution of standard deviation of v is similar. The global max value is 0.059 locating at the upper right corner, which is about 34% smaller than that of u. From Figures 2 to 5, the influence of uncertainty of velocity propagates with obvious directivity in the flow field. The convection effect of flow has the dominant contribution to the propagation of uncertainty.

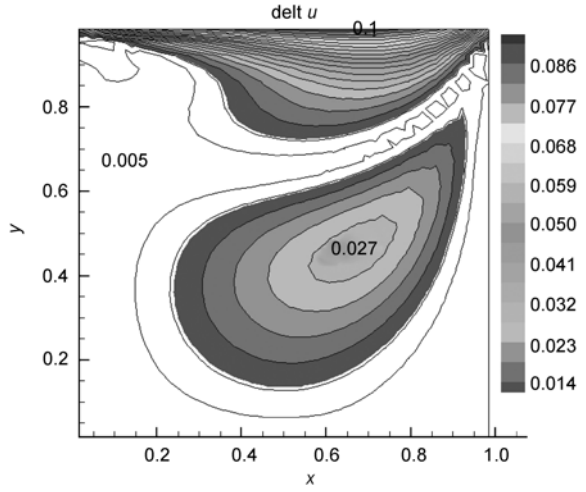

Figure 4 The contours of standard deviation of u (simulation 1).

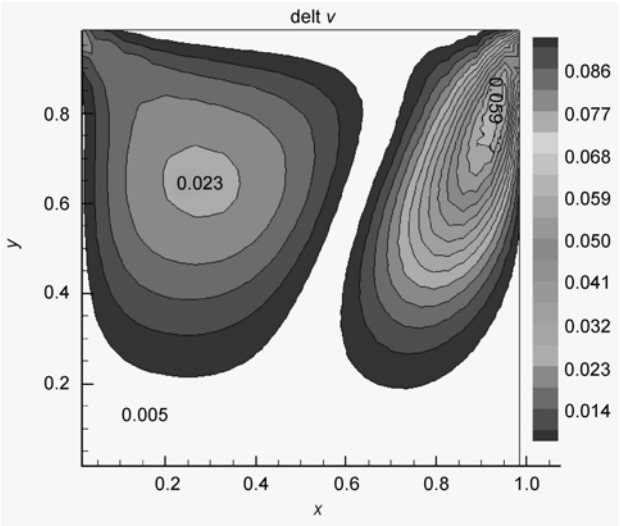

Figure 5 The contours of standard deviation of v (simulation 1).

4.2 Results of simulation 2

In ref. [12], the stochastic flow with uncertain flow viscosity was investigated and the standard deviation of velocity was shown. In this section, the investigation will be expanded with more details. The influences of uncertainty are different with different mean values of viscosity. Figure 6 shows the comparison of standard deviation of u at y = 0.5 for three different mean values of viscosity coefficients listed in simulation 2. As can be seen, in most range, the standard deviation for γ = 0.01 is much larger than those of other two. Furthermore, the standard deviation for γ = 0.05 is the second largest. The comparison of standard deviations of v at x = 0.5 is shown in Figure 7, which demonstrates the consistent results with Figure 6. It is easy to put forward the reason from the property of viscosity. With the increasing of fluid viscosity, the viscous force between the fluid particles increases. Then the capability of resistance of fluid increases. And the viscous diffusion increases which trends to make the flow field more uniform. Then, with the increasing

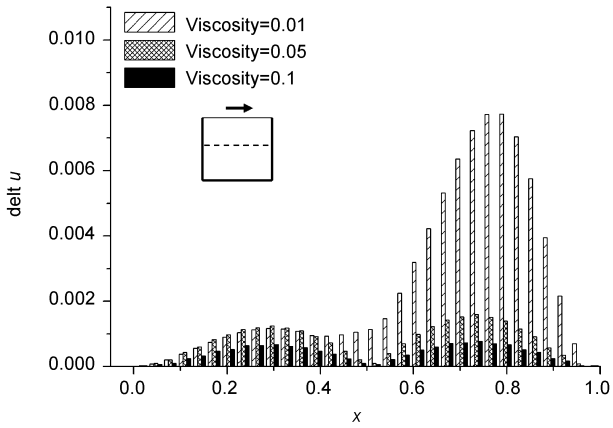

Figure 6 Comparison of standard deviations of u with different viscosity coefficients at y = 0.5.

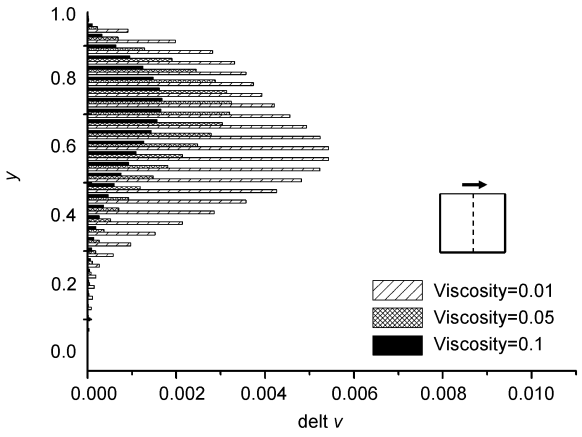

Figure 7 Comparison of standard deviations of v with different viscosity coefficients at x = 0.5.

of viscosity, the capability of resisting influence of uncertainty increases.

Figures 8 and 9 illustrate the contours of standard deviations of velocity components with $\gamma = 0.01$. Comparing these two figures with Figures 4 and 5, big differences can be seen from the distribution of standard deviation. There are three peaks of standard deviation which are distributed along the diagonal of the cavity decreasingly. The global max standard deviation is at the upper left corner with value 0.013. The standard deviation of v is less uniformly distributed with also three peaks. The global max value is 0.015, which is about 13% lower than that of u, with position near the right wall. Figure 10 shows the mean value of u at y = 0.5 with error bar. As can be seen from comparison with Figure 2, the profile of mean value is the same. However, the standard deviation in Figure 10 is much lower and without peaks overlapping as shown in Figure 2.

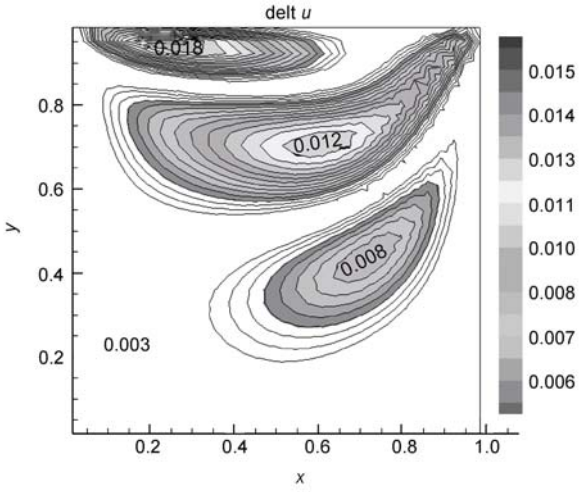

Figure 8 The contours of standard deviations of u (simulation 2).

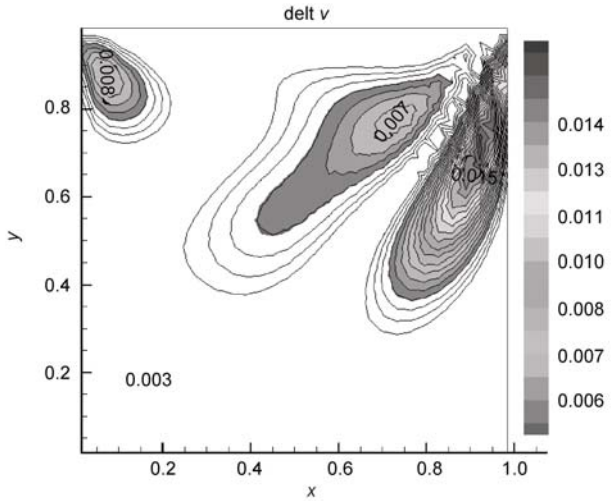

Figure 9 The contours of standard deviations of v (simulation 1).

4.3 Comparison of simulations 1 and 2

The comparison between the influence of uncertain boundary and uncertain flow property is presented below. The relative amplitudes of variation are the same. Results in simulation 2 with $\gamma = 0.01$, which has the biggest influence, is chosen. Figures 11 and 12 show the comparison of standard deviations of u at y = 0.5 and v at x = 0.5. As can be seen, in most range, the standard deviation of velocity with uncertain velocity boundary is much larger than that with uncertain viscosity, suggesting that the uncertain boundary has a larger influence. And the same conclusion as in the last subsection can be concluded that the convection effect has dominated contribution to the propagation of uncertain in the field, whereas the viscosity force has resistance effect on the propagation. Nevertheless, the coupled effect of uncertainties for multi-uncertainties problem and the influence of the grid independence should be investigated in a future work.

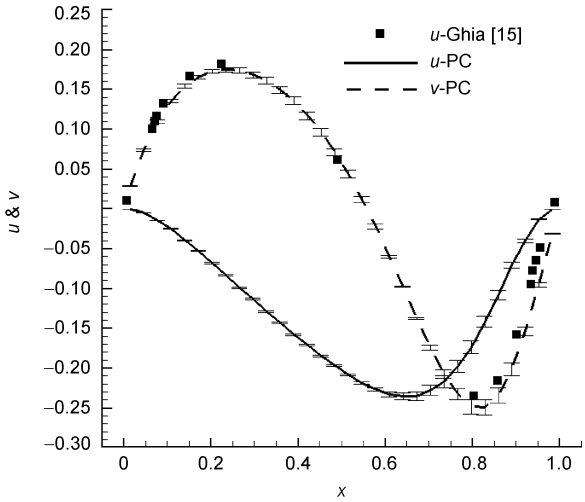

Figure 10 Distributions of mean values of velocity (simulation 2, at y = 0.5).

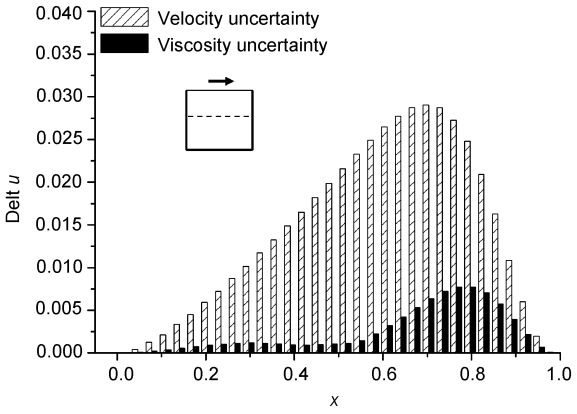

Figure 11 Comparison of standard deviations of u with different random variables at y = 0.5.

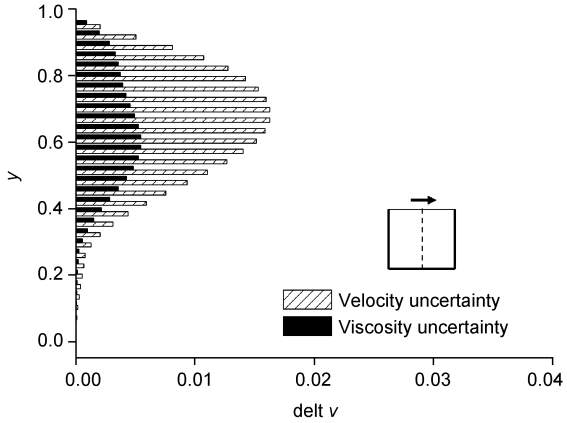

Figure 12 Comparison of standard deviations of v with different random variables at $x = 0.5$.

5 Conclusions

The polynomial chaos method was introduced into 2D laminar Navier-Stokes equation to simulate the non-deterministic behavior of lid driven cavity flow with influence of uncertain variables. The simulation results showed the effect of this method. The viscosity of fluid has resistance effect on propagation of uncertainty. The influence of random variables on flow parameters decreases with increasing of viscosity coefficient. For driven cavity flow, uncertain driven velocity has bigger influence than uncertain viscosity of fluid, even when *Re* number is very low.

This work was supported by the National Natural Science Foundation of China (Grant No. 90718025) and the EU Six Frame Project (Grant No. AST5-CT-2006-030959).

1 Chen Z B, Jiang X, Zhou Z, et al. Progress in application of CFD techniques. Sci China Ser E-Tech Sci, 2008, 51(7): 827–841
2 Oberkampf W L, Trucano T G. Guide for Verification and Validation of Computational Fluid Dynamics Simulation. Technical Report, AIAA, G-077. 1998
3 Kang S, Liu Q, Qi M X. CFD validation of a high speed centrifugal compressor impeller (in Chinese). J Eng Thermophys, 2005, 26(3): 400–404
4 Kang S. Influence of computational domain on CFD results (in Chinese). J Eng Thermophys, 2005, 26(Suppl): 57–60
5 European Commission (sixth framework). Non-deterministic Simulation for CFD-based Design Methodologies (NODESIM-CFD). EU Project, AST5-CT-2006-030959. 2006
6 Zang T, Hemsch M, Hilburger M, et al. Needs and Opportunities for Uncertainty Based Multidisciplinary Design Methods for Aerospace Vehicles. Hampton: NASA Langley Research Center, 2002
7 Wiener N. The homogeneous chaos. Am J Math,1938, 60: 897–936
8 Ghanem R G, Spanos P D. Stochastic Finite Elements: A Spectral Approach. Washington: Dover Publications, 2003
9 le Maitre O P, Knio O, Habib N N, et al. A stochastic projection method for fluid flow I. Basic formulation. J Comput Phys, 2001, 173: 481–511
10 Xiu D, Karniadakis G E. The Wiener-Askey polynomial chaos for stochastic differential equations. SIAM J Sci Comput, 2002, 24: 619–644
11 Xiu D, Karniadakis G E. Modeling uncertainty in flow simulations via generalized polynomial chaos. J Computl Phys, 2003, 187: 137–167
12 Lacor C, Smirnov S. Uncertainty propagation in the solution of compressible Navier-Stokes equations using polynomial chaos decomposition. In: NATO AVT Symposium, Athens, Greece, 2007
13 Wu H. Application of generalized polynomial chaos in stochastic differential equation (in Chinese). Dissertation of Doctoral Degree. Xi'an: Xi'an Jiaotong University, 2008
14 Wang X D, Kang S. Solving stochastic Burgers equation using polynomial chaos decomposition (in Chinese). J Eng Thermophys, 2010, 31(3): 393–398
15 Ghia U, Ghia K N, Shin C T. High-*Re* solutions for in-compressible flow using the Navier-Stokes equations and a multigrid method. J Comput Phys, 1982, 48: 387–411
16 Chen X J, Qin G L, Xu Z. Spectral element method and high order time splitting method for Navier-Stokes equation (in Chinese). Chin J Comput Mech, 2002, 19(3): 281–285